Brain
Pathology

Reduction in miR-219 expression underlies cellular pathogenesis of oligodendrocytes in a mouse model of Krabbe disease

Naoko Inamura[1] | Shinji Go[2] | Takashi Watanabe[2] | Hiroshi Takase[3] |
Nobuyuki Takakura[4] | Atsuo Nakayama[1,5] | Hirohide Takebayashi[6] | Junko Matsuda[2] |
Yasushi Enokido[1] 🟢

[1]Department of Cellular Pathology, Institute for Developmental Research, Aichi Developmental Disability Center, Kasugai, Japan

[2]Department of Pathophysiology and Metabolism, Kawasaki Medical School, Kurashiki, Japan

[3]Core Laboratory, Nagoya City University Graduate School of Medical Science, Nagoya, Japan

[4]Department of Signal Transduction, Research Institute for Microbial Diseases, Osaka University, Suita, Japan

[5]Department of Neurobiochemistry, Nagoya University School of Medicine, Nagoya, Japan

[6]Division of Neurobiology and Anatomy, Graduate School of Medical and Dental Sciences, Niigata University, Niigata, Japan

Correspondence
Yasushi Enokido, Department of Cellular Pathology, Institute for Developmental Research, Aichi Developmental Disability Center, 713-8 Kamiya-cho, Kasugai 480-0392, Aichi, Japan.
Email: enokido@inst-hsc.jp

Abstract

Krabbe disease (KD), also known as globoid cell leukodystrophy, is an inherited demyelinating disease caused by the deficiency of lysosomal galactosylceramidase (GALC) activity. Most of the patients are characterized by early-onset cerebral demyelination with apoptotic oligodendrocyte (OL) death and die before 2 years of age. However, the mechanisms of molecular pathogenesis in the developing OLs before death and the exact causes of white matter degeneration remain largely unknown. We have recently reported that OLs of twitcher mouse, an authentic mouse model of KD, exhibit developmental defects and endogenous accumulation of psychosine (galactosylsphingosine), a cytotoxic lyso-derivative of galactosylceramide. Here, we show that attenuated expression of microRNA (miR)-219, a critical regulator of OL differentiation and myelination, mediates cellular pathogenesis of KD OLs. Expression and functional activity of miR-219 were repressed in developing twitcher mouse OLs. By using OL precursor cells (OPCs) isolated from the twitcher mouse brain, we show that exogenously supplemented miR-219 effectively rescued their cell-autonomous developmental defects and apoptotic death. miR-219 also reduced endogenous accumulation of psychosine in twitcher OLs. Collectively, these results highlight the role of the reduced miR-219 expression in KD pathogenesis and suggest that miR-219 has therapeutic potential for treating KD OL pathologies.

KEYWORDS
demyelination, globoid cell leukodystrophy, Krabbe disease, lysosomal storage disease, microRNA, oligodendrocyte

---

Shinji Go and Takashi Watanabe are contributed equally to this work.

- -

1 | INTRODUCTION

Krabbe disease (KD), or globoid cell leukodystrophy, is an autosomal recessive lysosomal storage disease affecting nervous system white matter (1–3). Before 6 months of age, most KD patients (85%–90% of known cases) present with "infantile" or "classic" disease manifestations, such as extreme irritability, spasticity, and developmental delay. Severe motor and mental deterioration are also observed that lead to decerebration and death by 2 years of age. KD is caused by inherited mutations of the *GALC* gene encoding the lysosomal enzyme galactosylceramidase, which catalyzes the breakdown of galactosylceramide, a major myelin lipid in developing oligodendrocytes (OLs).

Over the last four decades, it has been shown that many cellular events, including OL death, neuronal atrophy, extensive astrogliosis, microglial activation, and the appearance of large, multinucleated phagocytes (globoid cells), are implicated in the pathology of the KD brain (4–6). It has been postulated that the loss of GALC activity in myelin-forming cells prompts them to accumulate endogenous psychosine (galactosylsphingosine), a highly cytotoxic lyso-derivative of galactosylceramide, which triggers widespread demyelination and subsequent neuropathological events (7, 8). However, although the dysfunction and cell death of OLs are likely the primary cause of demyelination in the KD brain, pathophysiological changes in OLs before death and white matter degeneration are still poorly understood, and the effective therapies for KD are yet to be established.

MicroRNAs (miRs) are a class of small non-coding RNAs composed of 19–24 nucleotides that induce RNA silencing by promoting its cleavage, poly(A) tail shortening, or by attenuating its translation by the ribosomes (9, 10). MicroRNAs act as regulators of cellular functions in health and disease. Among them, miR-219 was identified as a necessary and sufficient regulator of OL development, myelination, and remyelination (11, 12). Recent studies have shown that miR-219 is expressed specifically in differentiating OLs. miR-219 stimulates OL maturation by repressing the expression of genes encoding OL differentiation-inhibiting factors, such as *Pdgfra* and *Sox6* (11–13). Deletion of miR-219 leads to OL differentiation defects and impaired myelination of the developing CNS, indicating the physiological significance of miR-219 (13). Meanwhile, the pathological significance of miR-219 in myelin diseases has been suggested by the studies of demyelination experimentally induced by chemical (lysolecithin and cuprizone) and immunological (experimental allergic encephalomyelitis) methods in the models of multiple sclerosis (13–16), or by the transduction with Theiler's murine encephalomyelitis virus in a model of the virus-induced encephalomyelitis (17). However, although these pathological studies support the therapeutic effects of miR-219 on the remyelination of OLs in immune-mediated, non-cell-autonomous demyelination, the role of miR-219 in the pathogenesis of congenitally impaired OLs with cell-autonomous defects has not been investigated.

Recently, by using twitcher mice, an authentic mouse model of KD, and cultured OLs purified from the twitcher mouse brain, we have demonstrated that KD OLs exhibit cell-autonomous developmental defects and undergo apoptotic death associated with the aberrant accumulation of endogenous psychosine (18). In the present study, to develop our understanding of the mechanisms underlying KD OL pathology, we further investigated the role of miR-219 in the cellular pathogenesis of developing twitcher mouse OLs.

2 | MATERIALS AND METHODS

2.1 | Animals

The heterozygous twitcher mice (C57BL/6J, $Galc^{+/twi}$) were obtained from the Jackson Laboratory (Bar Harbor, ME, USA). They were crossed to generate wild-type ($Galc^{+/+}$) and the homozygous twitcher ($Galc^{twi/twi}$) mice used in this study. Genotypes were determined as previously described (19). The primers for genotyping were as follows: sense, 5′-cacttaattttctccagtcat-3′ and antisense, 5′-tagatggcccactgtcttcaggtgata-3′. All animal experiments were approved by the Institutional Animal Care and Use Committee (approval No. 2019-19) and the Institutional Biosafety Committee for Living Modified Organisms (approval No. 20-3) of the Aichi Developmental Disability Center, and performed in accordance with the Guidelines of Regulations and Guidelines of Animal Care and Use established by the Science Council of Japan and the ARRIVE guidelines. All mice were bred and housed in specific-pathogen-free conditions on a 12 h light/dark cycle (temperature 23 ± 1°C; humidity 40–60%; lights on from 07:00 to 19:00 h) with free access to food (CE-2, CLEA Japan, Inc., Tokyo, Japan) and water. For *in situ* hybridization, mice of both sexes at postnatal day 21 (P21) were anesthetized by the inhalation of vaporized isoflurane (4% induction, 2% maintenance), and transcardially fixed with 4% paraformaldehyde in 0.1 M phosphate buffer (pH 7.2), and the brain was dissected out. For western blotting and real-time quantitative reverse transcription PCR (qRT-PCR), mice of both sexes at P21 were anesthetized by 4% isoflurane and sacrificed by decapitation, and the brain was dissected out. For cell culture, wild-type and twitcher littermates of both sexes at P8–9 were sacrificed by decapitation, and the brains were isolated.

2.2 | Immunocytochemistry

Cultured cells were fixed with 4% paraformaldehyde in 0.1 M phosphate buffer pH 7.4 for 30 min, washed three

times with PBS containing 0.1% Triton X-100 (PBST), and further incubated with primary antibodies in PBST containing 2% BSA overnight at 4°C. The dilution conditions of primary antibodies for immunostaining were as follows: rabbit anti-Olig2 (AB9610, Merck Millipore, Burlington, MA, USA, 1:500), goat anti-myelin basic protein (MBP) (sc-13914, Santa Cruz Biotechnology, Dallas, TX, USA, 1:200), rabbit anti-cleaved caspase-3 (#9661, Cell Signaling Technology, Danvers, MA, USA, 1:400) and goat anti-Sox10 (sc-17342, Santa Cruz Biotechnology, 1:100). The cells were then incubated with secondary antibodies of Alexa Fluor 488- or 568-labeled anti-IgGs (Thermo Fisher Scientific, Waltham, MA, USA, 1:500) in PBST containing 2% BSA for 2 h at room temperature. Cells were counterstained with DAPI for nuclear staining, if necessary, and mounted for microscopic observations. Fluorescent images were acquired using a fluorescent microscope (BZ-9000, Keyence, Osaka, Japan).

2.3 | Western blotting

Cultured cells were washed three times with ice-cold PBS and dissolved in lysis buffer containing 62.5 mM Tris-HCl pH 6.8, 2% (w/v) SDS, 2.5% (v/v) 2-mercaptoethanol, and 5% (v/v) glycerol. Protein concentration was quantified by the BCA method (Pierce BCA Protein assay Kit; Thermo Fisher Scientific). The protein samples were subjected to electrophoresis (5 μg protein/lane) on an SDS-polyacrylamide gel and electroblotted onto a polyvinylidene difluoride membrane (Merck Millipore). The membrane was blocked with 5% globulin-free BSA (Wako Chemicals, Tokyo, Japan) in TTBS (20 mM Tris-HCl, pH 7.4, 150 mM NaCl, and 0.1% Tween 20), and incubated with primary antibody overnight at 4°C. The dilution conditions of primary antibodies for Western blotting were as follows: rabbit anti-cleaved caspase-3 (#9661, Cell Signaling Technology, 1:1000), goat anti-MBP (sc-13914, Santa Cruz Biotechnology, 1: 500), rabbit anti-proteolipid protein 1 (PLP; ab28486, Abcam, 1:500), and mouse anti-GAPDH (MAB374, Millipore, 1:10,000). Then, the membranes were incubated with peroxidase-conjugated anti-goat, -mouse or -rabbit secondary antibody (Kirkegaard and Perry Laboratories Inc., Gaithersburg, MD, USA, 1:5000) in TTBS, and immunoreactivity was visualized with Western BLoT Quant HRP Substrate (TAKARA Bio Inc., Tokyo, Japan) according to the manufacture's protocol, and chemiluminescence signals were digitized with ImageQuant LAS 4000 (GE Healthcare, Chicago, IL, USA). The expression levels of GAPDH of each protein sample were served as a loading control. Densitometric measurement of bands on western blotting was performed using ImageJ software (NIH Image, Bethesda, MD, USA).

2.4 | Cell culture

In vitro culturing and transfection experiments were performed with OPCs isolated from P8–9 mouse cortices and hippocampi by immunopanning with antibodies against PDGFRα (558774, BD Pharmingen, San Diego, CA, USA), as previously described (11, 20) with some modifications. Mouse brain tissues were enzymatically dissociated with papain (Worthington Biochemical, Lakewood, NJ, USA, 9 U/ml) for 30 min at 37°C, and positively immunopanned for PDGFRα after depletion of microglia with BSL1 (Vector Laboratories, Burlingame, CA, USA, 2.5 μg/ml). OPC purity was routinely determined by immunostaining for PDGFRα and Olig2, and exceeded 97%. Cells were plated at $2–5 × 10^4$ cells/cm^2 and grown in serum-free media, but with the addition of 1% N21-MAX Media Supplement (R&D Systems, Minneapolis, MN, USA) as an alternative to the B27 supplement. Platelet-derived growth factor-AA (PDGF; Wako Chemicals, 10 ng/ml) and neurotrophin-3 (NT-3; Wako Chemicals, 5 ng/ml) were added to the media to proliferate OPCs, whereas PDGF and NT-3 were removed, and 1% fetal bovine serum, triiodothyronine (T3) (40 ng/ml; Sigma-Aldrich) and ciliary neurotrophic factor (CNTF; 10 ng/ml, Wako Chemicals) were added to the differentiation media for OL differentiation. For miRNA transfection experiments, 20 nM of miRIDIAN miRNA mimic (Dharmacon, Lafayette, CO, USA) for miR-219-5p (c-310578-05-0005) or scrambled negative control (CN-001000-01-05) were transfected at day 0 when the media is replaced to the differentiation media by using Lipofectamine RNAiMAX Transfection Reagent (13778, Thermo Fisher Scientific) according to the manufacturer's protocol. In immunostaining experiments, 10 nM of BLOCK-iT™ Alexa Fluor™ Red Fluorescent Control (1475100, Thermo Fisher Scientific) was co-transfected with each miRNA mimic to allow the identification of transfected cells.

2.5 | RNA extraction and qRT-PCR

Total RNA was extracted from cultured cells and brain tissues with ISOGEN II (NIPPON GENE Co Ltd, Toyama, Japan) or miRNeasy Mini Kit (QIAGEN, Hilden, Germany) according to the manufacturer's protocol. The cortical gray matter and corpus callosum (1 to 4 mm anterior to lambda) were sliced by an Acrylic Coronal Brain Slicer (MK-MC-01, Muromachi Kikai Co., Ltd, Tokyo, Japan) and trimmed with a sharpened tungsten needle. Four animals were analyzed for each genotype. For cDNA synthesis of mRNAs, 100 ng of total RNA was reverse transcribed using ReverTra Ace® qPCR RT Master Mix (TOYOBO Co., Ltd, Osaka, Japan) according to the manufacturer's protocol. For cDNA synthesis of miR-NAs, 100 ng of total RNA was reverse transcribed

using MystiCq® microRNA cDNA Synthesis Mix (Sigma-Aldrich) according to the manufacturer's protocol. Quantifications of mRNA and miRNA levels were performed with a CFX96™ Real-Time PCR Detection System (Bio-Rad, Hercules, CA, USA) using SYBR Green fluorescence detection and melting curve analysis. The forward and reverse primer sets used for mRNA analysis were as follows: *Mbp* (NM_010777.3, 411–512) (21): 5′-ggcctcagaggacagtgatg-3′ (forward) and 5′-tctgctgtgtgcttggagtc-3′ (reverse); *Plp1* (NM_011123.3, 542–659) (21): 5′-gttccagaggccaacatcaagctc-3′ (forward) and 5′-agccatacaacagtcagggcatag-3′ (reverse) and *Gapdh* (12): 5′-gtgtgaaccacgagaaata-3′ (forward) and 5′-gttgtcatggatgacctt-3′ (reverse). PCR products derived from each primer set were checked for purity and appropriate size by polyacrylamide gel electrophoresis. RT-qPCR of miRNA was performed using 10 nM of each MystiCq® microRNA qPCR Assay Primer (Sigma-Aldrich) for miR-16 (MIRAP00029), miR-219 (MIRAP00276) and RNU6 (MIRCP00001) and of MystiCq® Universal PCR Primer (MIRUP-500RXN). mRNA and miRNA expression levels were determined by the SYBR Green-based qRT-PCR assay with THUNDERBIRD® SYBR qPCR Mix (TOYOBO Co., Ltd) according to the manufacturer's protocol. PCR thermal cycling conditions were as follows: 95°C for 60 s, followed by 40 cycles of 95°C for 15 s and 60°C for 60 s. The final melting curve analysis (65–95°C, increment/0.5°C for 5 s) was routinely performed as an indicator of amplicon specificity. Relative expression levels of each target mRNA and miRNA were determined by comparing threshold cycles for individual products normalized by the expression levels of *Gapdh* mRNA (for mRNA quantification) or RNU6 snRNA (for miRNA quantification) using the $2^{-\Delta\Delta CT}$ method (22). Data analysis was carried out by CFX Manager Software (Bio-Rad).

2.6 | miRNA *in situ* hybridization

In situ hybridization of miRNA was performed using a modified *in situ* protocol (23) with DIG-labeled miR-CURY LNA™ detection probes (QIAGEN) for miR-219 (miRCURY LNA Detection probe #619109-360) and Scramble-miR negative control (miRCURY LNA Detection Control probe #699004-360). Paraffin-embedded mouse brain sections (10 μm) were deparaffinized and rehydrate, and then incubated with 10 μg/ml of proteinase K (P4850, Sigma-Aldrich) at 37°C for 10 min. Washed sections with PBS were incubated in imidazole buffer [0.13 M 1-methylimidazole (Wako Chemicals), 300 mM NaCl, pH 8.0], followed by an incubation in EDC-Imidazole solution [0.16 M 1-ethyl-3-(3–dimethyl aminopropyl) carbodiimide (Tokyo Chemicals, Tokyo, Japan) in imidazole buffer, pH 8.0] for 2 h at room temperature. After washing the sections, 25 nM DIG-labeled

probe in G-Hybo-L hybridization buffer (GenoStuff, Tokyo, Japan) was hybridized to each section overnight. The hybridization temperature = DNA *Tm* probe −20–21°C. For probe detection, washed sections were incubated with alkaline phosphatase-conjugated anti-DIG antibody (1:1,000, Roche, Basel, Switzerland) in Blocking buffer [1% Blocking reagent (Roche), 150 mM NaCl, 100 mM Tris-Cl, pH7.5] overnight at 4°C. Washed sections with TBST (50 mM Tris-HCl, 150 mM NaCl, 0.1% Tween 20, pH 7.5) were soaked in Staining Buffer (100 mM NaCl, 100 mM Tris-HCl, 50 mM $MgCl_2$, pH9.5), followed by an incubation with NBT/BCIP solution (1:50, Roche) in Staining Buffer at room temperature. Slides were then washed in PBS and water, and mounted for color bright-field microscopic observations using a Keyence BZ-9000 microscope equipped with a 20 × objective. miR-219-positive (miR-219$^+$) cells were counted in the region between 3 and 4 mm anterior to lambda as follows: for the corpus callosum, the counted cells were within the coronal section 1 mm from the midline, whereas for the cortical gray matter, the cells were counted within the parasagittal section 1 to 2 mm from the midline. The cells were assessed in at least four microscopic visual fields in one tissue section using five brain sections per animal. Four animals were analyzed for each genotype.

2.7 | Luciferase reporter assay

Cells in a 48-well culture plate were transfected using Lipofectamine 3000 (L3000001, Thermo Fisher Scientific) with 1 μg of pmirGLO Dual-Luciferase reporter (E1330, Promega, Madison, WI, USA) containing two expression units, that encode Renilla luciferase (*Rluc*) used as a transfection control for normalization and firefly luciferase (*Fluc*) with the segments of targeted seed sequence of miR-219 or its mismatch mutant in the 3′-UTR, respectively, used as the primary reporter to monitor the miRNA functional activity for inhibiting mRNA translation. The segments were cloned into the PmeI-XbaI site of pmirGLO vector, and NotI site at position 93 in the vector was added for clone confirmation, according to the manufacture's protocol. Sequences added in the vector were as followed: miR-219 sense: 5′-aaactagcggccgctagtagaattgcgtttggacaatcat-3′; miR-219 antisense: 5′-ctagatgattgtccaaacgcaattctactagcggccgcta gttt-3′; miR-219 mismatch mutant sense: 5′-aaactagcggcc gctagtagaattgcgtttggccgcggat-3′; miR-219 mismatch mutant antisense: 5′-ctagatccgcggccaaacgcaattctactagcggcc gctagttt-3′. Seventy-two hours after transfection with the miR-219 pmirGLO vector constructs, cells were analyzed for luciferase activity using the Dual-Luciferase Assay System (E2920, Promega) and a Gene Light® luminometer (Microtech Co., Ltd, Tokyo, Japan). Normalized firefly luciferase activity (Fluc activity/Rluc activity) for each construct was compared to that transfected with

pmirGLO vector no-insert control as 100% to evaluate the inhibitory effect of miR-219 on its targets.

2.8 | Psychosine quantitation

Psychosine levels of the primary cultured KD OLs (at day 4) from twitcher mice were determined by the high-performance liquid chromatography (HPLC), using the method described previously (18, 24). Cultured cells were detached from the culture plate by the treatment of Accutase™ (Innovative Cell Technologies, San Diego, CA, USA) for 40 min at room temperature, and harvested by centrifugation at 1500 g for 10 min. In brief, 300 μl of chloroform/methanol (1:2, v/v) containing 40 pmol of eicosasphinganine (Matreya LLC, State College, PA, USA) as an internal standard, were added to cell pellet, and thoroughly mixed for 30 s and kept for 30 min at room temperature, and was centrifuged at 1500 g for 10 min. The supernatant was collected and evaporated under nitrogen flow at 37°C. The sample was saponified in 250 μl of chloroform/methanol (1:2, v/v) containing 0.1 N NaOH, by incubation at 37°C for 2 h. The saponified sample was partitioned by adding 25 μl of chloroform/methanol (1:2, v/v), 250 μl of chloroform, and 100 μl of water. After centrifuging at 1500 g for 10 min, the upper aqueous phase was discarded and the lower organic phase was washed with chloroform/methanol/0.8 mM NH_4OH (3:48:47, v/v). The remained lower phase was evaporated and dissolved in 50 μl of methanol. The dissolved lipid solution was mixed with o-phthalaldehyde derivatization reagent (3% potassium borate (pH 10.5) solution containing 0.5 mg/ml of OPA, 1% ethanol, and 0.05% mercaptoethanol) and incubated for 15 min at room temperature. The reaction was stopped by the addition of 0.5 ml of mobile phase (methanol/5 mM sodium phosphate, pH 7.0 containing 50 mg/L of sodium octylsulfate, 14:1, v/v) for HPLC. The HPLC analysis was conducted with a C18 column (TSKgel ODS-100 V; 4.6 mm i.d. ×250 mm, Tosoh, Tokyo, Japan) and the isocratic mobile phase at the flow rate of 0.6 ml/min. The OPA derivatives were detected with a fluorescence detector (excitation wavelength 340 nm, emission wavelength 455 nm). The peaks of psychosine were quantitated from the fluorescence level of standard psychosine (Sigma-Aldrich), and corrected by the recovery ratio of the internal standard eicosasphinganine and expressed in pmol/μg protein.

2.9 | Statistical analysis

Statistical significance was evaluated using the Student's *t*-test to compare differences between the two groups and two-way ANOVA with Bonferroni *post hoc* test for multiple comparisons. Data represent the mean ± standard error of the mean (SEM). A *p* value less than 0.05 was considered statistically significant.

3 | RESULTS

3.1 | Expression and functional activity of miR-219 are repressed in developing twitcher OLs

miR-219 is expressed specifically and robustly in OLs of the developing brain (11, 12, 25). To investigate whether the expression of miR-219 is affected in the developing twitcher mouse brain, we performed *in situ* hybridization of miR-219, focusing on the corpus callosum region of wild-type and twitcher littermates at postnatal day 21 (P21), when OL differentiation and myelination take place most actively (Figure 1A) (26, 27). The number of miR-219-positive (miR-219^{+}) cells in twitcher mice was significantly reduced by 20–30% compared to that in wild-type mice (Figure 1B, *p* < 0.05). qRT-PCR analysis confirmed the reduction of miR-219 expression in twitcher mouse revealed by *in situ* hybridization (Figure 1C, *p* < 0.01), whereas no significant difference between the two genotypes was observed in the level of miR-16 (*p* = 0.75), an endogenous housekeeping miRNA (28). In line with the observations in the corpus callosum, fewer miR-219^{+} cells were detected in the cortical gray matter (Figure S1) and other white matter brain areas in twitcher mice (Figure 1D).

Next, to investigate whether the expression level of miR-219 is reduced specifically in twitcher mouse OLs, we examined miR-219 levels in differentiating OLs of wild-type and twitcher littermates. OL precursor cells (OPCs) purified from the brains of wild-type and twitcher littermates were cultured in the differentiation medium for 1–5 days and then, the level of miR-219 was detected by qRT-PCR. We found that the expression of miR-219 in differentiating twitcher OLs was significantly lower than in wild-type OLs (Figures 2A, 3 and 5 days, *p* < 0.01, respectively), whereas the levels of miR-16 expression were not significantly different. Then, by the luciferase reporter assay, we examined whether the functional activity of miR-219, namely the inhibitory effect on mRNA translation, was affected in twitcher OLs. In wild-type OLs, the luminescent activity of the reporter encoded by the firefly luciferase (*Fluc*) mRNA was twofold lower if it carried a miR-219-targeted seed sequence in the 3′-UTR compared to the level obtained in the case of the control no-insert pmirGLO vector (Figure 2B, *p* < 0.01). This effect was abolished when the reporter carried a mismatch mutant seed sequence. Meanwhile, the suppression of Fluc luminescence in twitcher OLs was weaker than that in wild-type OLs, indicating that the functional activity of miR-219 was repressed in twitcher OLs in accordance with its reduced expression.
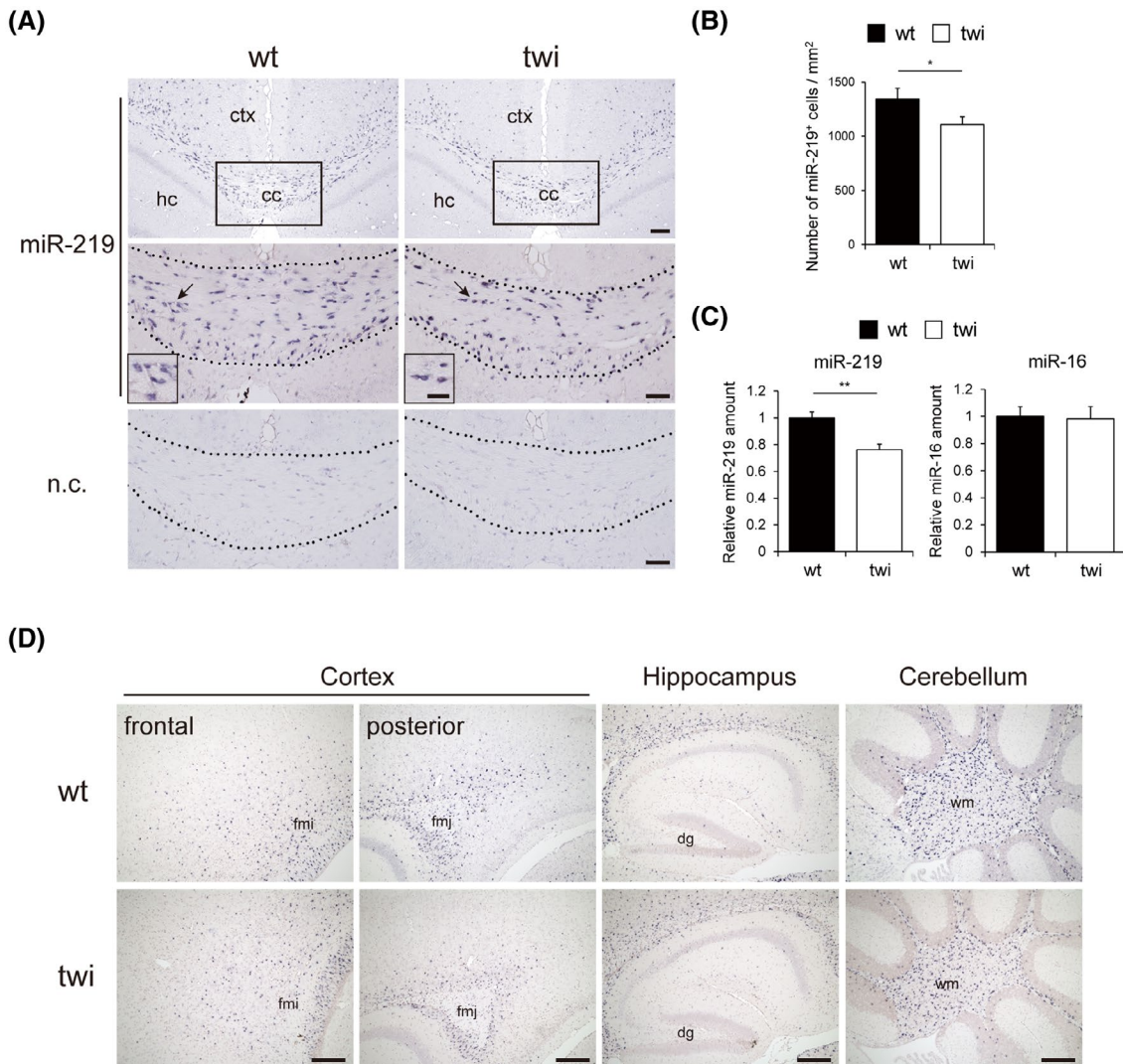
FIGURE 1 Reduced expression of miR-219 in developing twitcher mouse brain. (A) *In situ* hybridization images showing miR-219-positive (miR-219$^+$) cells in coronal sections of wild-type (wt) and twitcher (twi) mouse brain at postnatal day 21 (P21), compared to the expression of a scramble negative control (n.c.) miRNA probe. Boxed corpus callosum regions in the upper panel are shown at higher magnification in the middle panel. Scale bars, 100 μm in the upper panel and 50 μm in the middle and lower panels. cc, corpus callosum; ctx, cortex; hc, hippocampus. Dotted lines indicate the cc boundary. Insets, High-magnification images showing miR-219$^+$ cells around the areas of arrows. Scale bar: 25 μm. (B) Quantification of miR-219$^+$ cells per mm^2 in the corpus callosum of wt and twi mice at P21. Data are presented as the mean ± SEM of four animals per genotype. *$p < 0.05$; Student's *t*-test. (C) qRT-PCR analysis showing the expression levels of miR-219 and miR-16 in the corpus callosum of twi mice relative to those in wt littermates; total RNA preparations from mice of both genotypes at P21 were used. Expression levels are presented as ratios of miRNA amounts relative to the respective mean levels in the samples from wt mice. Data are presented as the mean ± SEM of four animals per genotype. **$p < 0.01$; Student's *t*-test. (D) *In situ* hybridization images of miR-219$^+$ cells in different brain regions in sagittal sections of wt and twi mouse brain at P21. Scale bars: 200 μm. dg, dentate gyrus; fmi, forceps minor corpus callosum; fmj, forceps major corpus callosum; wm, white matter

3.2 | Exogenous miR-219 supplementation rescues cellular pathologies of twitcher OLs.

We have recently reported that OLs of twitcher mice exhibit cell-autonomous developmental defects and undergo apoptotic death upon endogenous psychosine accumulation (18). To investigate whether reduced expression of miR-219 is implicated in these pathological changes, we examined the effect of exogenous supplementation with miR-219 on differentiating twitcher OLs. Purified OPCs transfected with either a synthetic

nucleotide molecule homologous to the mature miR-219 (miR-219 mimic) or scrambled negative control miRNA (n.c.) were cultured for 4 days in the differentiation media and then, differentiated OLs were detected by immunostaining for myelin basic protein (MBP), a mature oligodendrocyte marker (Figure 3A). The number of MBP$^+$ cells was significantly lower in cultured twitcher OLs transfected with the n.c. than in cultured wild-type OLs (Figure 3B, wt + n.c. vs. twi + n.c., $p < 0.01$). However, in cultured twitcher OLs transfected with the miR-219, the number of MBP$^+$ cells,

(A)
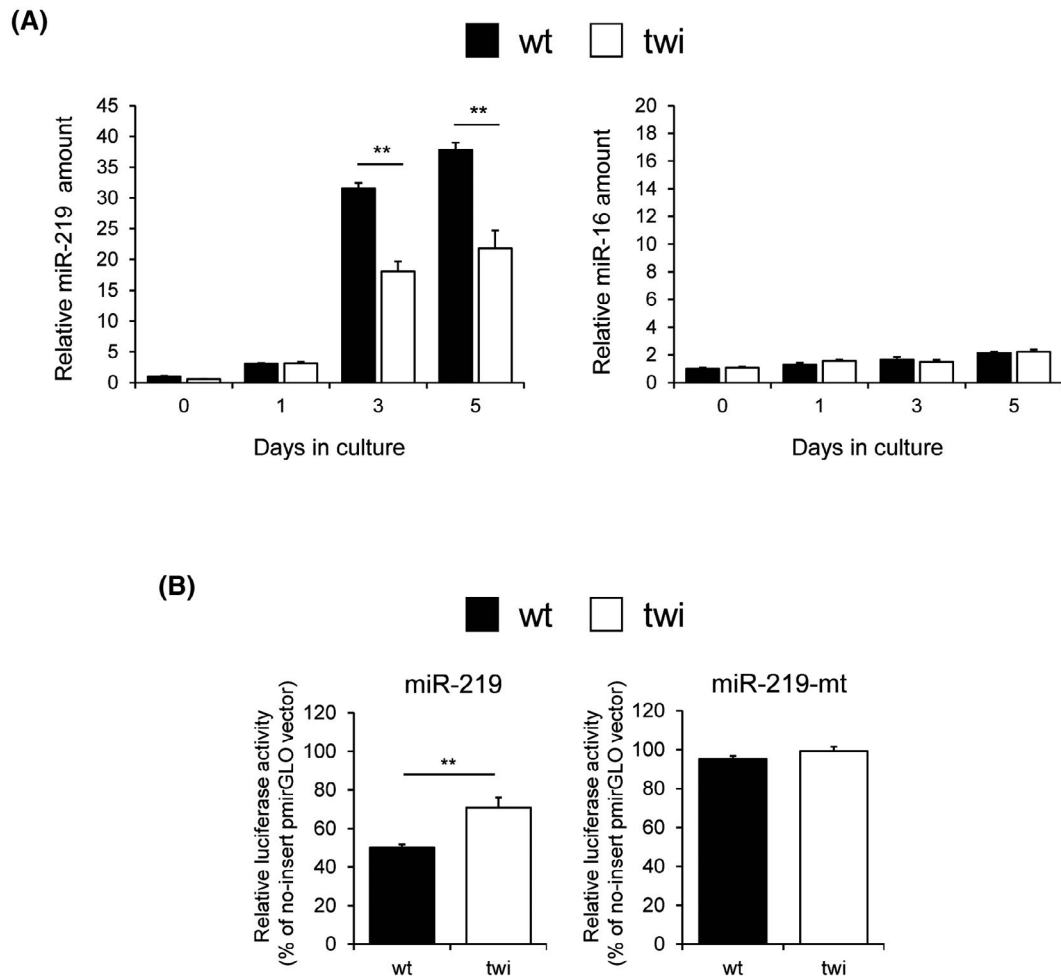
■ wt □ twi

(B)

■ wt □ twi

FIGURE 2 Reduced expression and functional activity of miR-219 in developing twitcher OLs. (A) qRT-PCR analysis showing the expression levels of miR-219 and miR-16 in differentiating primary OLs of twi mice relative to those in wt animals; total RNA preparations from purified OPCs cultured for 0, 1, 3 or 5 days in the differentiating medium were used. Expression levels are presented as ratios relative to the mean level in wt samples at day 0. Data are presented as the mean ± SEM (n = 3). **$p < 0.01$; two-way ANOVA with Bonferroni *post hoc* test. (B) Luciferase reporter assay showing the reduced functional activity of miR-219 in primary OLs of twitcher mice relative to those in wt animals. Purified OPCs isolated from wt and twi mouse were transfected with pmirGLO vectors containing two expression units that encode firefly luciferase (Fluc) carrying the segment of the miR-219-targeted seed sequence (miR-219) or its mismatch mutant (miR-219-mut) in the 3′-UTR. Fluc was used as the primary reporter to monitor the functional activity of miR-219 for suppressing mRNA expression, whereas Renilla luciferase (Rluc) acted as transfection control. Normalized firefly luciferase activity (Fluc activity/Rluc activity) for each construct was compared to that in cells transfected with pmirGLO vector no-insert control as 100% to evaluate the functional activity of miR-219 on its targets. Transfected cells were cultured for 72 h in the differentiating medium and then analyzed for luciferase activity by the dual-luciferase assay. Data are presented as the mean ± SEM ($n = 4$). **$p < 0.01$; Student's *t*-test

as well as the relative mRNA (Figure 3C) and protein (Figure 3D,E) expression levels of the myelin markers MBP and proteolipid protein (PLP), were markedly recovered (twi + n.c. vs. twi + miR-219, $p < 0.01$) (Figure 3B,C,E), and comparably increased to those of wild-type OLs.

We next asked if apoptotic death of OLs, which is the main cause of demyelination in KD, could also be rescued by miR-219. Purified OPCs from wild-type and twitcher mice were transfected with either miR-219 or n.c., cultured for 4 days in the differentiation medium, and then immunostained for cleaved caspase-3, a marker of apoptotic cells (Figure 4A). The number of apoptotic cells was significantly higher among cultured twitcher

OLs transfected with n.c. relative to that among cultured wild-type OLs (Figure 4B, wt + n.c. vs. twi + n.c., $p < 0.01$). However, in cultured twitcher OLs transfected with miR-219, the number of apoptotic cells was markedly reduced (twi + n.c. vs. twi + miR-219, $p < 0.01$), and became comparable to those in cultured wild-type OLs (wt + n.c. vs. twi + miR-219 and wt + miR-219 vs. twi + miR-219, $p = 0.53$ and $p = 0.27$, respectively). This was further confirmed by western blotting (Figure 4C,D). In comparison with wild-type OLs transfected with n.c., the protein level of cleaved caspase-3 was markedly increased in twitcher OLs with n.c. (wt + n.c. vs. twi + n.c., $p < 0.01$), and this was comparably reduced in twitcher OLs transfected with miR-219 (twi + n.c. vs.
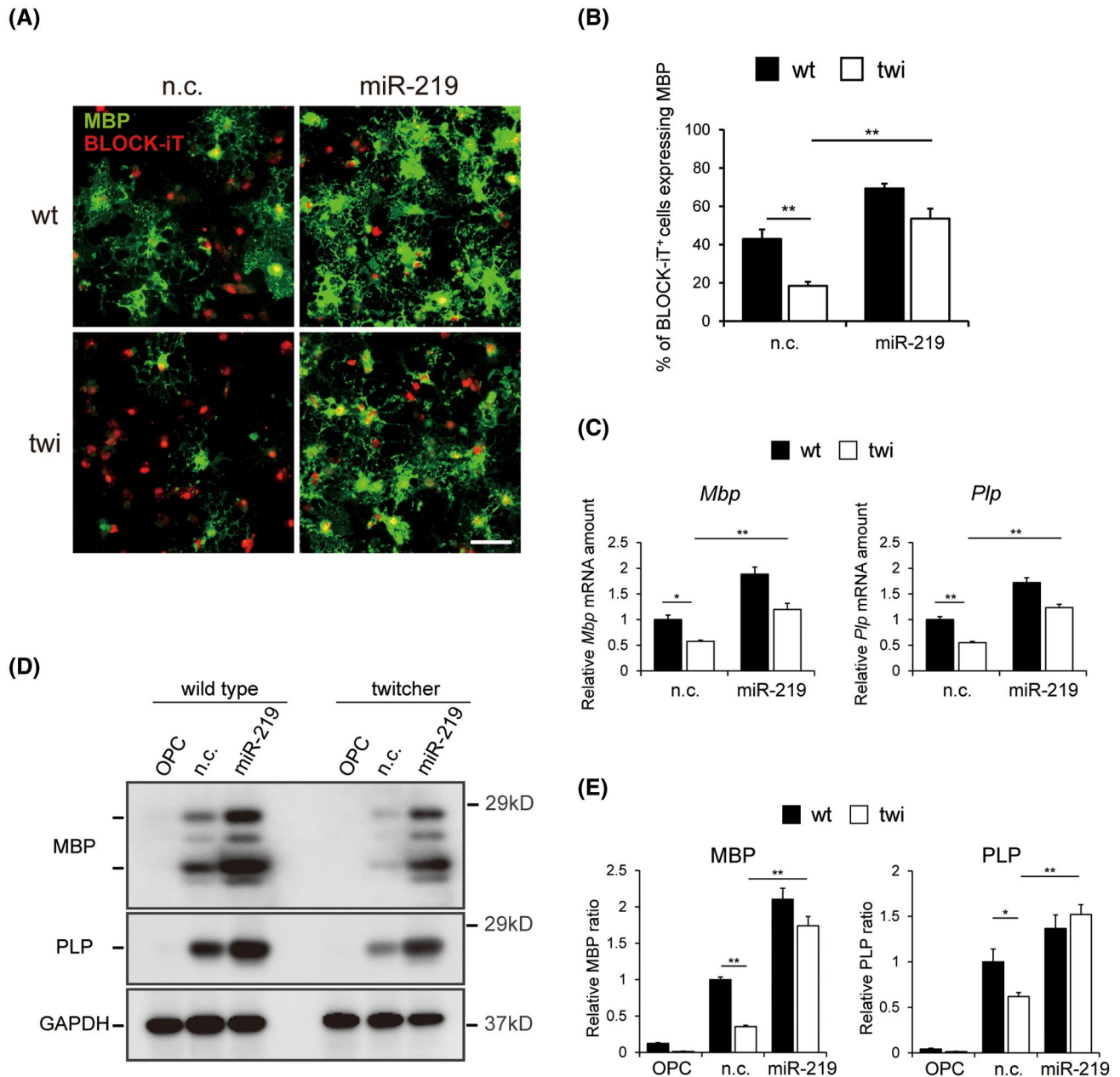
(A)

(B)

(C)

(D)

(E)

FIGURE 3 Effect of miR-219 on the development of twitcher OLs. (A) OPCs isolated from wild-type (wt) and twitcher (twi) pups were cultured in the differentiating medium for 4 days with miRNA negative control (n.c.) or miR-219. Differentiated OLs were immunostained for MBP (MBP⁺ cells, green). The miRNA-transfected cells were identified by the expression of BLOCK-iT™ Alexa Fluor™ Red Fluorescent Control (BLOCK-iT⁺ cells, red). Scale bar: 50 μm. (B) Percentages of MBP⁺ cells transfected with n.c. or miR-219 among total Block-iT⁺ cells after 4 days of culturing in the differentiating medium. Data are presented as the mean ± SEM ($n = 3$). **$p < 0.01$; two-way ANOVA with Bonferroni *post hoc* test. (C) qRT-PCR analysis showing the expression levels of *Mbp* and *Plp* mRNAs in primary twi OLs relative to those in wt OLs transfected with n.c. or miR-219. Total RNA preparations from primary OLs cultured for 4 days in differentiating medium were used. Expression levels are presented as ratios relative to the respective mean amount in untreated wt OLs. Data are presented as the mean ± SEM ($n = 3$). *$p < 0.05$, **$p < 0.01$; two-way ANOVA with Bonferroni *post hoc* test. (D) Western blot image showing the expression levels of MBP and PLP proteins in differentiating OLs of wt and twi mice transfected with n.c. or miR-219; protein lysates from differentiating OLs cultured for 4 days in the differentiating medium were used. MBP blot shown is a stripped and reprobed blot of the loading control (GAPDH). Representative blots from three independent experiments are shown. (E) Band intensities MBP and PLP in (D) were normalized to the corresponding loading control. Expression levels are presented as ratios of protein amounts relative to those in samples from n.c. transfected wild-type OLs. Data represent the mean ± SEM ($n = 3$). *$p < 0.05$, **$p < 0.01$; two-way ANOVA with Bonferroni *post hoc* test

twi + miR-219, $p < 0.01$; wt + n.c. vs. twi + miR-219 and wt + miR-219 vs. twi + miR-219, $p = 0.07$ and $p = 0.57$, respectively).

We further examined the effect of miR-219 on the level of endogenous psychosine in twitcher OLs. We have previously reported that psychosine levels in the twitcher
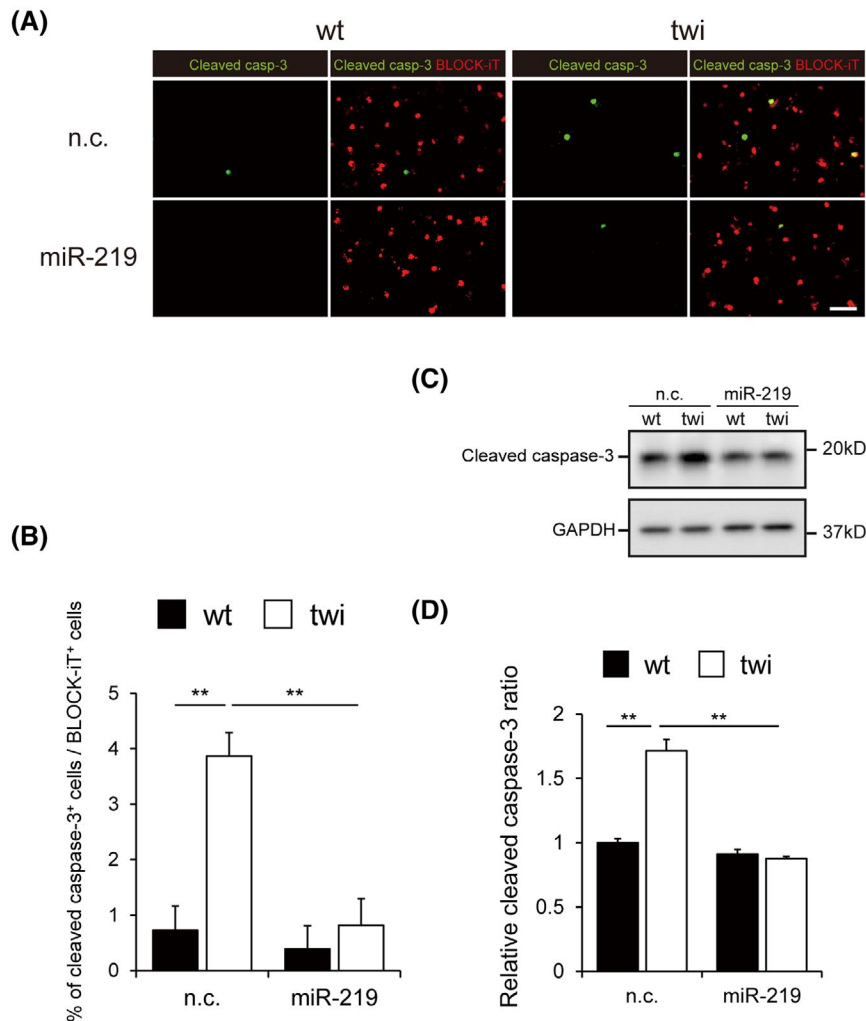
FIGURE 4 Effect of miR-219 on apoptotic cell death of twitcher OLs. (A) OPCs isolated from wild-type (wt) and twitcher (twi) pups were cultured in the differentiating medium for 4 days with miRNA negative control (n.c.) or miR-219. Cells immunostained for cleaved caspase-3 (green) were considered apoptotic. The miRNA-transfected cells were identified by the expression of BLOCK-iT™ Alexa Fluor™ Red Fluorescent Control (red). Scale bar: 50 μm. (B) Percentages of cleaved caspase-3$^+$ cells transfected with n.c. or miR-219 among total Block-iT$^+$ cells after culturing for 4 days in the differentiating medium. Data are presented as the mean ± SEM ($n = 3$). **$p < 0.01$; two-way ANOVA with Bonferroni *post hoc* test. (C) Western blot image showing the expression levels of cleaved caspase-3 in differentiating OLs of wt and twi mice transfected with n.c. or miR-219; protein lysates from differentiating OLs cultured for 4 days in the differentiating medium were used. Blot shown is a stripped and reprobed blot of the loading control (GAPDH). Representative blots from three independent experiments are shown. (D) Band intensities of cleaved caspase-3 in (C) were normalized to the corresponding loading control. Expression levels are presented as ratios of protein amounts relative to those in samples from n.c. transfected wild-type OLs. Data represent the mean ± SEM ($n = 3$). **$p < 0.01$; two-way ANOVA with Bonferroni *post hoc* test

mouse brain and purified OLs similarly increased during development, whereas in wild-type animals, psychosine levels were barely detectable (18, 24, 29). Interestingly, although it was hard to observe the effect of miR-219 on the level of psychosine in wild-type OLs (wt + n.c., 0.138 ± 0.031 pmol/μg protein; wt + miR-219, 0.109 ± 0.031 pmol/μg protein, $p = 0.87$), the abnormally increased level of psychosine in twitcher OLs was partially but significantly reduced by the transfection with miR-219 (Figure 5, wt + n.c. vs. twi + n.c. and twi + n.c. vs. twi + miR-219, $p < 0.01$).

Taking into account these results and the reduced expression and functional activity of miR-219 in developing twitcher OLs, we concluded that the dysregulation of miR-219 underlies the cellular pathogenesis of KD OLs, and its exogenous supplementation has an ameliorative effect on KD OL pathologies.

4 | DISCUSSION

Pathophysiological significance of miR-219 in diseases involving myelin impairment has been suggested by the studies of experimentally induced non-cell autonomous demyelination (13–17). However, the cell-autonomous pathogenic role of miR-219 in diseased OLs has remained largely unknown. In this study, we explored the role of miR-219 in the cell-autonomous OL pathogenesis in KD,
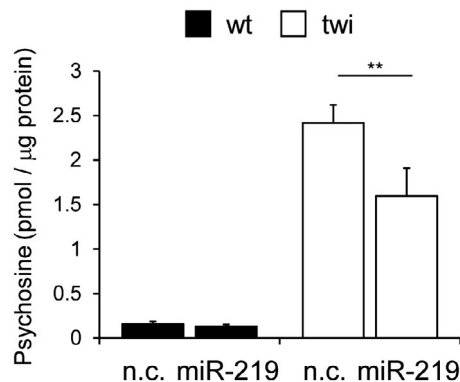
FIGURE 5 Effect of miR-219 on endogenous psychosine accumulation in twitcher OLs. Bar graphs of psychosine levels in differentiated wild-type (wt) and twitcher (twi) OLs transfected with miRNA negative control (n.c.) or miR-219. Data are presented as the mean ± SEM ($n = 7$). **$p < 0.01$; two-way ANOVA with Bonferroni *post hoc* test

an inherited lysosomal storage disease with progressive demyelination and apoptotic OL death. We show that the expression and functional activity of miR-219 are repressed in OLs of twitcher mice, an authentic mouse model of KD, and that cell-autonomous pathology of purified twitcher OLs is rescued by exogenous supplementation with miR-219. Our findings provide new insights into the role of miR-219 in developing OLs in health and disease and its therapeutic potential for the treatment of OL pathologies in KD.

miR-219 is a necessary and sufficient regulator of OL differentiation, myelination, and remyelination (11–13, 25). Although loss-of-function mutations of the majority of individual miRNAs cause no overt developmental defects in many organisms (30), genetic deletion of miR-219 leads to defective OL development and high susceptibility to the experimentally induced demyelinating lesions (13). However, the roles of miR-219 in the pathogenesis of developing OLs have not been fully elucidated. By using OLs purified from the brains of twitcher mice, we have demonstrated previously that KD OLs exhibit developmental defects and abnormal myelin formation (18), which precede the characteristic KD pathologies of progressive OL death and demyelination. Our present results extend this notion by showing that the reduction of miR-219 expression plays a pathogenic role in developing KD OLs.

Previous studies have suggested that the inhibitors of the psychosine-synthesizing pathway, L-cycloserine and carmofur, may be utilized as drugs against KD (31–34). L-Cycloserine is an inhibitor of serine palmitoyltransferase, a rate-limiting enzyme for *de novo* synthesis of sphingolipids, including psychosine. Carmofur directory inhibits the lysosome-specific acid ceramidase ASAH1, which has been recently reported to catalyze psychosine formation through the catabolic deacylation of galactosylceramide. Both L-cycloserine and carmofur reduce psychosine accumulation in KD cells, although they

have only limited efficacy in OL pathologies (32, 33). In this regard, it should be noted that both enzymes are involved in sphingolipid metabolism under normal conditions; therefore, their inhibition alters the metabolic balance of other important lipids (35–37). In fact, mutations in the palmitoyltransferase subunit SPTLC1 cause hereditary sensory neuropathy type I with prominent sensory involvement and a variable degree of motor and autonomic dysfunction (38, 39). Moreover, a defect in the activity of ASAH1 causes Farber disease (FD) characterized by deformed joints, progressive hoarseness, subcutaneous nodules, and neurologic deterioration (40, 41). Importantly, despite psychosine accumulation and inflammatory manifestations caused by the twitcher mutation were successfully counteracted in the twitcher × FD model mouse cross, the overall phenotype was indistinguishable from that of the FD parental line (33). In addition, it has been known that a serious adverse effect of carmofur is the induction of leukoencephalopathy characterized by progressive damage to the white matter in the brain (42). Because sphingolipids are fundamental myelin components, and developing OLs require large amounts of sphingolipids for myelin formation (43), these findings collectively suggest that inhibitors of sphingolipid metabolism may adversely affect proper OL differentiation and myelination in the developing brain. In contrast to these agents, miR-219 improves myelin formation and survival of developing OLs in the absence of apparent negative side effects, which makes it a possible candidate therapeutic for the treatment of KD.

The underlying mechanisms of the ameliorative effects of miR-219 on the cellular pathology of developing twitcher OLs are currently unclear. In the present study, we have shown that miR-219 reduced psychosine accumulation in developing twitcher OLs (Figure 5). Recent studies have shown that psychosine preferentially accumulates in membrane microdomains in the brain of KD patients and twitcher mice, leading to the disruption of lipid rafts that play a crucial role in membrane trafficking and cell signaling (44–47). In addition, it has been known that psychosine mediates apoptotic cell death via caspase-3 activation in various cell types (45, 48–50). The reduction in the endogenous psychosine level by miR-219 could contribute to the function and stabilization of myelin and to the suppression of caspase-3 activation in differentiating twitcher OLs. The next challenges are the detailed clarification of the underlying mechanisms of these actions and elucidation of the ways how miR-219 expression and function are modulated in developing KD OLs. In addition, further *in vivo* studies should be performed to examine whether exogenous supplementation with miR-219 suppresses a sequence of OL pathologies in the twitcher mouse brain.

In conclusion, our experiments using primary OLs purified from an authentic mouse model of KD suggest that the deficit in miR-219, a specific miRNA regulating OL development, is implicated in the pathogenesis

of the cell-autonomous demyelinating disease. Our results suggest that the elucidation of the mechanisms underlying the therapeutic effect of miR-219 in various disease conditions as well as understanding the processes regulating miR-219 expression and function may further broaden our knowledge about the role of miRNA disturbances in the molecular pathogenesis of myelin diseases from biological and clinical standpoints.

CONFLICT OF INTEREST

The authors have no conflicts of interest to declare.

AUTHOR CONTRIBUTIONS

Naoko Inamura performed experiments, designed figures, and contributed to the interpretation of results and design of the project. Hiroshi Takase, Atsuo Nakayama, and Nobuyuki Takakura performed experiments and provided expertise in the interpretation of histological or cytological results. Shinji Go, Takashi Watanabe, Hirohide Takebayashi, and Junko Matsuda provided mice, performed experiments, and discussed overall results. Yasushi Enokido designed the project, oversaw all aspects of it, performed experiments, and co-wrote the manuscript. All authors read and approved the final manuscript.

DATA AVAILABILITY STATEMENT

The data that support the findings of this study are available from the corresponding author upon reasonable request.

ORCID

Yasushi Enokido https://orcid.org/0000-0003-3252-504X

REFERENCES

1. Krabbe K. A new familial, infantile form of brain sclerosis. Brain. 1916;39:74–114.
2. Suzuki K. Globoid cell leukodystrophy (Krabbe's disease): update. J Child Neurol. 2003;18:595–603.
3. Wenger DA, Rafi MA, Luzi P, Datto J, Costantino-Ceccarini E. Krabbe disease: genetic aspects and progress toward therapy. Mol Genet Metab. 2000;70:1–9.
4. Graziano AC, Cardile V. History, genetic, and recent advances on Krabbe disease. Gene. 2015;555:2–13.
5. Suzuki K. Twenty-five years of the "psychosine hypothesis": a personal perspective of its history and present status. Neurochem Res. 1998;23:251–9.
6. Taniike M, Mohri I, Eguchi N, Irikura D, Urade Y, Okada S, et al. An apoptotic depletion of oligodendrocytes in the twitcher, a murine model of globoid cell leukodystrophy. J Neuropathol Exp Neurol. 1999;58:644–53.
7. Igisu H, Suzuki K. Progressive accumulation of toxic metabolite in a genetic leukodystrophy. Science. 1984;224:753–5.
8. Miyatake T, Suzuki K. Globoid cell leukodystropy: additional deficiency of psychosine galactosidase. Biochem Biophys Res Commun. 1972;48:538–43.
9. Bartel DP. MicroRNAs: target recognition and regulatory functions. Cell. 2009;136:215–33.
10. Rupaimoole R, Slack FJ. MicroRNA therapeutics: towards a new era for the management of cancer and other diseases. Nat Rev Drug Discov. 2017;16:203–22.
11. Dugas JC, Cuellar TL, Scholze A, Ason B, Ibrahim A, Emery B, et al. Dicer1 and miR-219 are required for normal oligodendrocyte differentiation and myelination. Neuron. 2010;65:597–611.
12. Zhao X, He X, Han X, Yu Y, Ye F, Chen Y, et al. MicroRNA-mediated control of oligodendrocyte differentiation. Neuron. 2010;65:612–26.
13. Wang H, Moyano AL, Ma Z, Deng Y, Lin Y, Zhao C, et al. miR-219 cooperates with miR-338 in myelination and promotes myelin repair in the CNS. Dev Cell. 2017;40:566–82.
14. Fan HB, Chen LX, Qu XB, Ren CL, Wu XX, Dong FX, et al. Transplanted miR-219-overexpressing oligodendrocyte precursor cells promoted remyelination and improved functional recovery in a chronic demyelinated model. Sci Rep. 2017;7:41407.
15. Liu S, Ren C, Qu X, Wu X, Dong F, Chand YK, et al. miR-219 attenuates demyelination in cuprizone-induced demyelinated mice by regulating monocarboxylate transporter 1. Eur J Neurosci. 2017;45:249–59.
16. Pusic AD, Kraig RP. Youth and environmental enrichment generate serum exosomes containing miR-219 that promote CNS myelination. Glia. 2014;62:284–99.
17. Moyano AL, Steplowski J, Wang H, Son KN, Rapolti DI, Marshall J, et al. microRNA-219 reduces viral load and pathologic changes in Theiler's virus-induced demyelinating disease. Mol Ther. 2018;26:730–43.
18. Inamura N, Kito M, Go S, Kishi S, Hosokawa M, Asai K, et al. Developmental defects and aberrant accumulation of endogenous psychosine in oligodendrocytes in a murine model of Krabbe disease. Neurobiol Dis. 2018;120:51–62.
19. Sakai N, Inui K, Tatsumi N, Fukushima H, Nishigaki T, Taniike M, et al. Molecular cloning and expression of cDNA for murine galactocerebrosidase and mutation analysis of the twitcher mouse, a model of Krabbe's disease. J Neurochem. 1996;66:1118–24.
20. Emery B, Dugas JC. Purification of oligodendrocyte lineage cells from mouse cortices by immunopanning. Cold Spring Harbor Prot; 2013;2013(9):854–68.
21. Lebrun-Julien F, Bachmann L, Norrmén C, Trötzmüller M, Köfeler H, Rüegg MA, et al. Balanced mTORC1 activity in oligodendrocytes is required for accurate CNS myelination. J Neurosci. 2014;34:8432–48.
22. Livak KJ, Schmittgen TD. Analysis of relative gene expression data using real-time quantitative PCR and the 2(-delta delta C(T)) method. Methods. 2001;25:402–8.
23. Pena JT, Sohn-Lee C, Rouhanifard SH, Ludwig J, Hafner M, Mihailovic A, et al. miRNA in situ hybridization in formaldehyde and EDC-fixed tissues. Nat Methods. 2009;6:139–41.

24. Matsuda J, Vanier MT, Saito Y, Tohyama J, Suzuki K, Suzuki K. A mutation in the saposin A domain of the sphingolipid activator protein (prosaposin) gene results in a late-onset, chronic form of globoid cell leukodystrophy in the mouse. Hum Mol Genet. 2001;10:1191–9.

25. Shin D, Shin JY, McManus MT, Ptácek LJ, Fu YH. Dicer ablation in oligodendrocytes provokes neuronal impairment in mice. Annal Neurol. 2009;66:843–57.

26. Bjelke B, Seiger A. Morphological distribution of MBP-like immunoreactivity in the brain during development. Int J Dev Neurosci. 1989;7:145–64.

27. Sturrock RR. Myelination of the mouse corpus callosum. Mol Genet Metab. 1980;6:415–20.

28. Landgraf P, Rusu M, Sheridan R, Sewer A, Iovino N, Aravin A, et al. A Mammalian microRNA expression atlas based on small RNA library sequencing. Cell. 2007;129:1401–14.

29. Ezoe T, Vanier MT, Oya Y, Popko B, Tohyama J, Matsuda J, et al. Twitcher mice with only a single active galactosylceramide synthase gene exhibit clearly detectable but therapeutically minor phenotypic improvements. J Neurosci Res. 2000;59:179–87.

30. Miska EA, Alvarez-Saavedra E, Abbott AL, Lau NC, Hellman AB, McGonagle SM, et al. Most *Caenorhabditis elegans* microRNAs are individually not essential for development or viability. PLoS Genet. 2007;3:e215.

31. Hawkins-Salsbury JA, Shea L, Jiang X, Hunter DA, Guzman AM, Reddy AS, et al. Mechanism-based combination treatment dramatically increases therapeutic efficacy in murine globoid cell leukodystrophy. J Neurosci. 2015;35:6495–505.

32. LeVine SM, Pedchenko TV, Bronshteyn IG, Pinson DM. L-cycloserine slows the clinical and pathological course in mice with globoid cell leukodystrophy (twitcher mice). J Neurosci Res. 2000;60:231–6.

33. Li Y, Xu Y, Benitez BA, Nagree MS, Dearborn JT, et al. Genetic ablation of acid ceramidase in Krabbe disease confirms the psychosine hypothesis and identifies a new therapeutic target. Proc Natl Acad Sci U S A. 2019;116:20097–103.

34. Ribbens JJ, Moser AB, Hubbard WC, Bongarzone ER, Maegawa GH. Characterization and application of a disease-cell model for a neurodegenerative lysosomal disease. Mol Genet Metab. 2013;111:172–83.

35. Kihara A. Synthesis and degradation pathways, functions, and pathology of ceramides and epidermal acylceramides. Prog Lipid Res. 2016;63:50–69.

36. Realini N, Solorzano C, Pagliuca C, Pizzirani D, Armirotti A, Luciani R, et al. Discovery of highly potent acid ceramidase inhibitors with in vitro tumor chemosensitizing activity. Sci Rep. 2013;3:1035.

37. Sundaram KS, Lev M. Inhibition of sphingolipid synthesis by cycloserine in vitro and in vivo. J Neurochem. 1984;42:577–81.

38. Bejaoui K, Wu C, Scheffler MD, Haan G, Ashby P, Wu L, et al. SPTLC1 is mutated in hereditary sensory neuropathy, type 1. Nat Genet. 2001;27:261–2.

39. Rotthier A, Auer-Grumbach M, Janssens K, Baets J, Penno A, Almeida-Souza L, et al. Mutations in the SPTLC2 subunit of serine palmitoyltransferase cause hereditary sensory and autonomic neuropathy type I. Am J Hum Genet. 2010;87:513–22.

40. Farber S. A lipid metabolic disorder: disseminated lipogranulomatosis; a syndrome with similarity to, and important difference from, Niemann-Pick and Hand-Schüller-Christian disease. Am J Dis Child. 1952;84:499–500.

41. Sugita M, Dulaney JT, Moser HW. Ceramidase deficiency in Farber's disease (lipogranulomatosis). Science. 1972;178:1100–2.

42. Yamada T, Okamura S, Okazaki T, Ushiroyama T, Yanagawa Y, Ueki M, et al. Leukoencephalopathy following treatment with carmofur: a case report and review of the Japanese literature. Asia-Oceania J Obst Gynaecol. 1989;15:161–8.

43. van Echten-Deckert G, Herget T. Sphingolipid metabolism in neural cells. Biochim Biophys Acta. 2006;1758:1978–94.

44. Abbandonato G, Storti B, Tonazzini I, Stöckl M, Subramaniam V, Montis C, et al. Lipid-conjugated rigidochromic probe discloses membrane alteration in model cells of Krabbe disease. Biophys J. 2019;116:477–86.

45. Hawkins-Salsbury JA, Parameswar AR, Jiang X, Schlesinger PH, Bongarzone E, Ory DS, et al. Psychosine, the cytotoxic sphingolipid that accumulates in globoid cell leukodystrophy, alters membrane architecture. J Lipid Res. 2013;54:3303–11.

46. Simons M, Krämer EM, Thiele C, Stoffel W, Trotter J. Assembly of myelin by association of proteolipid protein with cholesterol- and galactosylceramide-rich membrane domains. J Cell Biol. 2000;151:143–54.

47. White AB, Givogri MI, Lopez-Rosas A, Cao H, van Breemen R, Thinakaran G, et al. Psychosine accumulates in membrane microdomains in the brain of krabbe patients, disrupting the raft architecture. J Neurosc. 2009;29:6068–77.

48. Formichi P, Radi E, Battisti C, Pasqui A, Pompella G, Lazzerini PE, et al. Psychosine-induced apoptosis and cytokine activation in immune peripheral cells of Krabbe patients. J Cell Phys. 2007;212:737–43.

49. Giri S, Khan M, Rattan R, Singh I, Singh AK. Krabbe disease: psychosine-mediated activation of phospholipase A2 in oligodendrocyte cell death. J Lipid Res. 2006;47:1478–92.

50. Zaka M, Wenger DA. Psychosine-induced apoptosis in a mouse oligodendrocyte progenitor cell line is mediated by caspase activation. Neurosci Lett. 2004;358:205–9.

SUPPORTING INFORMATION

Additional Supporting Information may be found online in the Supporting Information section.

FIGURE S1 Reduced expression of miR-219 in the cortical gray matter in twitcher mouse brain. (A) *In situ* hybridization images showing miR-219-positive (miR-219^{+}) cells in sagittal sections of wild-type (wt) and twitcher (twi) mouse cortex at P21. Scale bar: 200 μm. Insets, High-magnification images showing miR-219^{+} cells in boxed cortical gray matter regions. Scale bar: 50 μm. (B) Quantification of miR-219^{+} cells per mm^2 in the cortical gray matter of wt and twi mice at P21. Data are presented as the mean ± SEM of four animals per genotype. *$p < 0.05$; Student's *t*-test. (C) qRT-PCR analysis showing the expression levels of miR-219 and miR-16 in mouse cortical gray matter of twi mice relative to those in wt littermates; total RNA preparations from mice of both genotypes at P21 were used. Expression levels are presented as ratios of miRNA amounts relative to the respective mean levels in the samples from wt mice. Data are presented as the mean ± SEM of four animals per genotype. **$p < 0.01$; Student's *t*-test